Supplement of Atmos. Chem. Phys., 23, 9495–9524, 2023
https://doi.org/10.5194/acp-23-9495-2023-supplement

Atmospheric Chemistry and Physics Open Access

Supplement of

Assimilation of POLDER observations to estimate aerosol emissions

Athanasios Tsikerdekis et al.

Correspondence to: Otto P. Hasekamp (o.p.hasekamp@sron.nl) and Athanasios Tsikerdekis (thanos.tsikerdekis@knmi.nl)

Table S1. List of selected meteorological and aerosol options of ECHAM-HAM used for the experiments.

Description (Reference)	Model Option
Horizontal resolution of 1.875°, corresponding to 192 x 96 grid cells. For RES_{LOW} only 3.75°	hres = T63
Vertical resolution of 31 hybrid sigma pressure levels up to 10hPa	vres = L31
Cumulus cloud convection scheme (Nordeng et al., 1994)	iconv = 1
Sub-grid-scale stratiform clouds scheme (Sundqvist et al., 1989)	icover = 1
Rapid Radiation Transfer Model for General circulation models (RRTM-G; Iacono et al., 2008)	-
Land surface model JSBACH (Reick et al., 2013)	-
Boundary layer parameterization (Stevens et al., 2013 and reference therenin)	-
Nudge vorticity, divergence, temperature and surface pressure to ERA5 reanalysis	-
Dust emission scheme (Stier et al., 2005) with updated East Asia soil properties	ndust = 4
Sea salt emission scheme (Long et al., 2011)	nseasalt = 7
Air-sea exchange parameterization for DMS emissions (Nightingale, 2000)	npist = 3
Kappa-Koehler theory for aerosol water growth (Petters and Kreidenweis, 2007)	nwater = 1
Size depended in-cloud and below-cloud scavenging (Tegen et al., 2019 and reference therein)	nwetdep = 3
Enable interactive dry deposition scheme (Tegen et al., 2019 and reference therein)	ndrydep = 1
Enable radiatively active aerosol	naerorad = 1

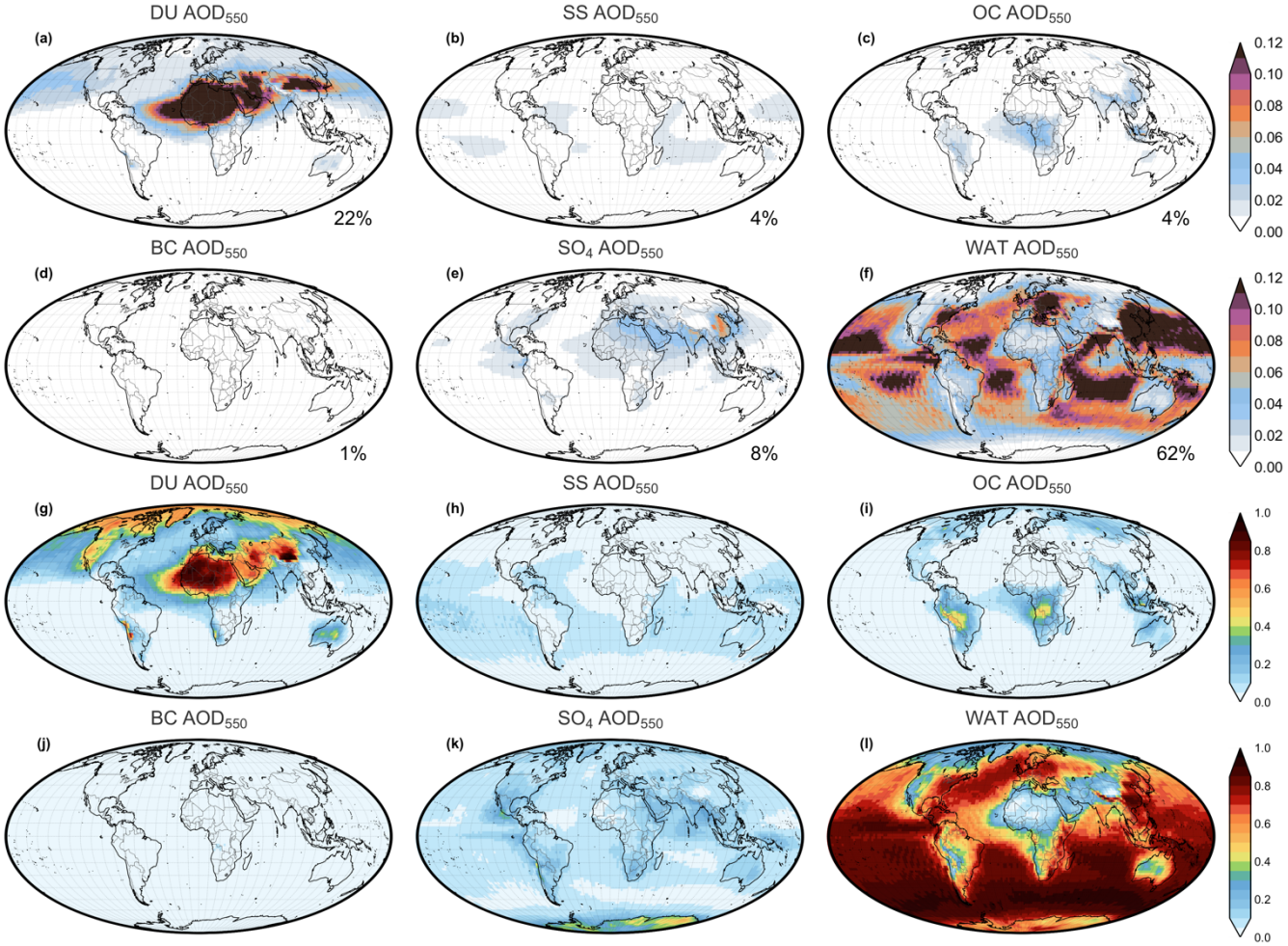

Figure S1. Optical depth at 550nm of CTL_{ECHAM} for (a) dust (DU), (b) sea salt (SS), (c) organic carbon (OC), (d) black carbon (BC), (e) sulphates (SO_4) and (f) water condensed on the surface of aerosol particles (WAT). The global contribution of each species to the total aerosol optical depth at 550nm is depicted at the right bottom corner. Third and fourth row depicts the contribution of each species to total aerosol optical depth at 550nm in each pixel.

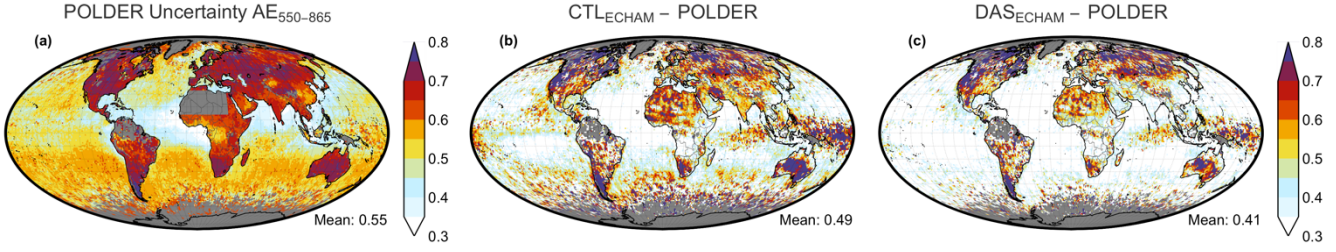

Figure S2. The (a) POLDER $AE_{550\text{-}865}$ uncertainty along with the averaged 3-hourly mean absolute error of $AE_{550\text{-}865}$ based on POLDER for (b) CTL_{ECHAM} and (c) DAS_{ECHAM}. The global mean is depicted at the right bottom corner of each plot.

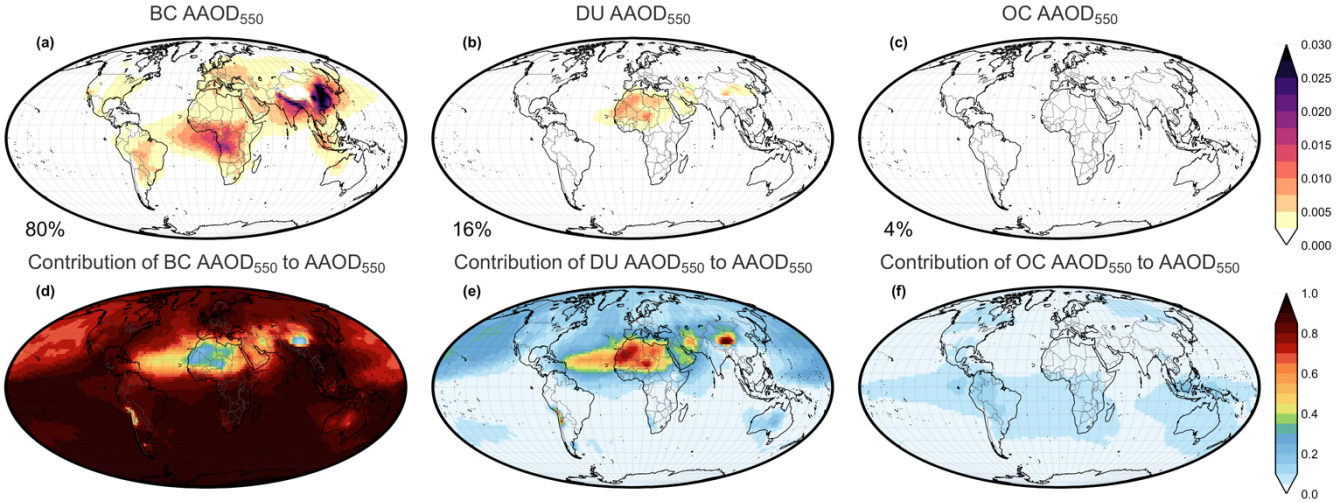

Figure S3. Absorption aerosol optical depth at 550nm ($AAOD_{550}$) of CTL_{ECHAM} for (a) black carbon, (b) dust and (c) organic carbon (first row), along with the contribution of each species to the total absorption aerosol optical depth at 550nm in each pixel (second row). The percentage in the bottom left corner indicates the global contribution of each species to $AAOD_{550}$.

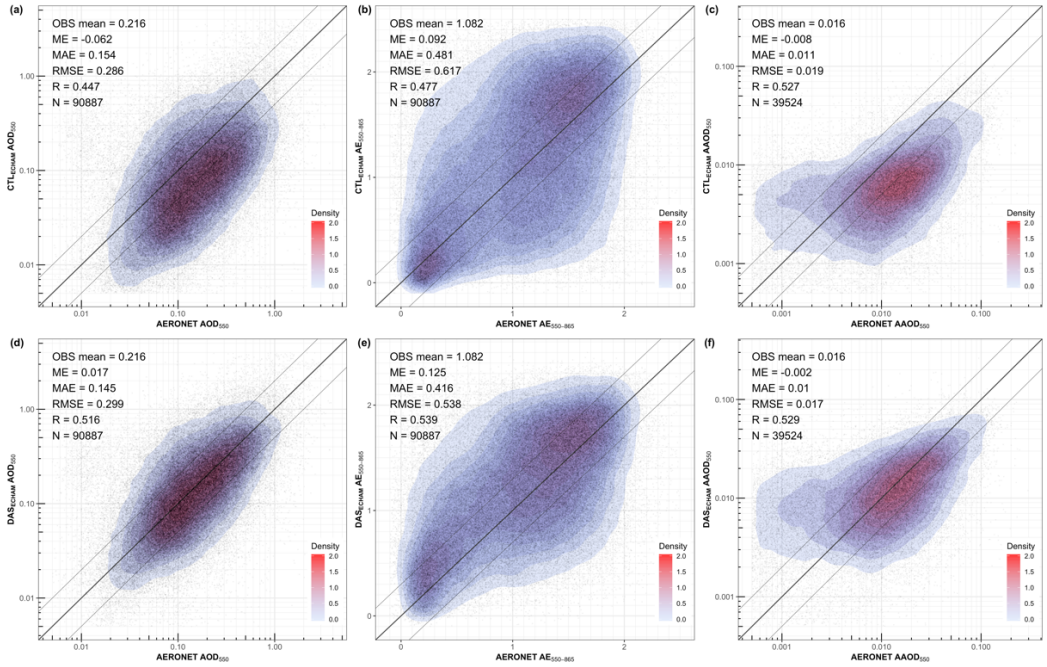

Figure S4. An evaluation of CTL_{ECHAM} and DASECHAM based on AERONET for the year 2006 (not collocated with POLDER). The first, second and third column corresponds to the variables AOD_{550}, $AE_{550\text{-}865}$ and $AAOD_{550}$ respectively. The Mean Error (ME), Mean Absolute Error (MAE), Root Mean Square Error (RMSE), Pearson Correlation (R) and the number of data points used in each case (N) is depicted at the top-left of each subplot. The AOD_{550} and $AE_{550\text{-}865}$ evaluation is based on AERONET Version 3 Direct Sun Algorithm Level 2.0, while the $AAOD_{550}$ and SSA_{550} evaluation is based on AERONET Version 3 Direct Sun and Inversion Algorithm Level 1.5.

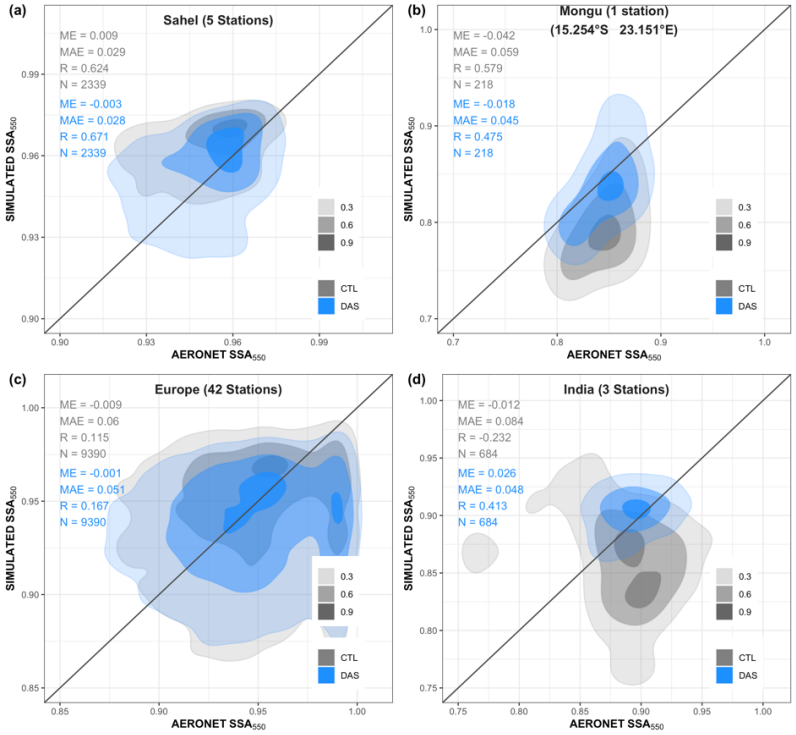

Figure S5. SSA_{550} evaluation of CTL_{ECHAM} and DAS_{ECHAM} based on selected AERONET sites (cyan points in Figure 2g) for the year 2006. These stations are selected over regions where natural and anthropogenic emissions of BC occur. The shaded areas depict the 2D density estimate scaled to a maximum of one for 0.3, 0.6 and 0.9 intervals. The Mean Error (ME), Mean Absolute Error (MAE), Pearson Correlation (R) and the number of data points used in each case (N) is depicted for each subplot. The evaluation is based on AERONET Version 3 Direct Sun and Inversion Algorithm Level 1.5.

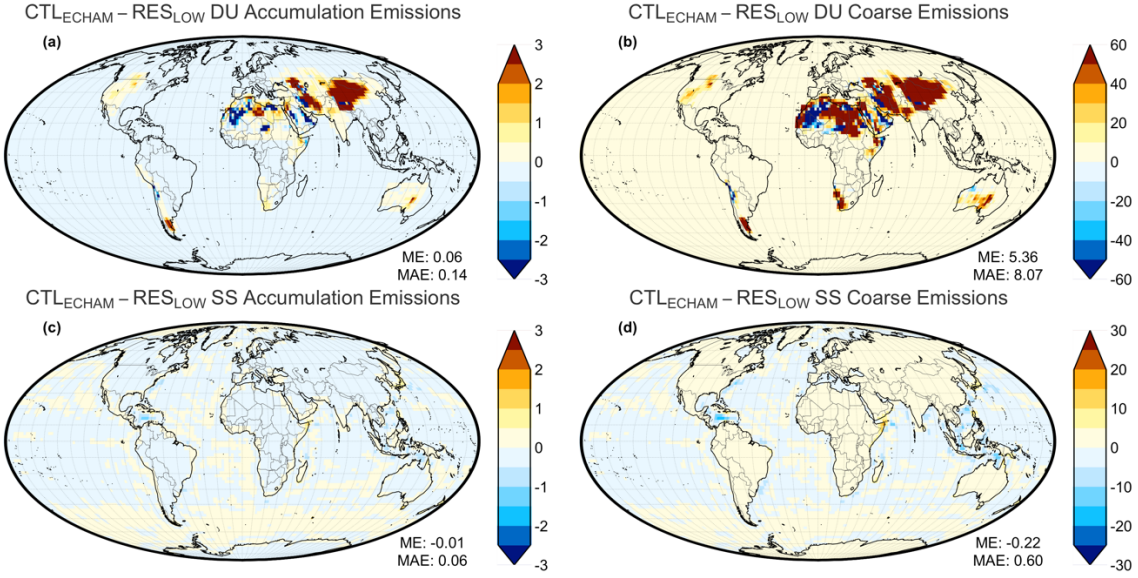

Figure S6. Differences of $CTL_{ECHAM} - RES_{LOW}$ for dust (DU) and sea salt (SS) emissions. The global mean error (ME) and the global mean absolute error (MAE) is depicted at the right bottom corner of each plot.

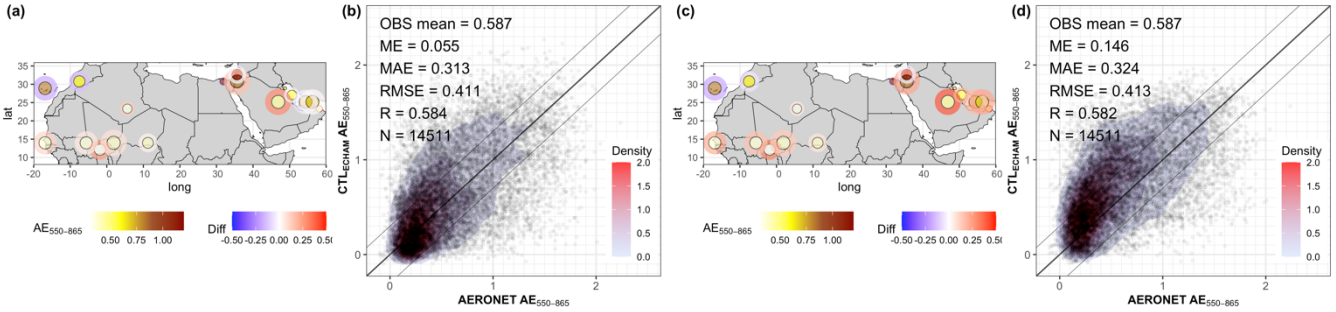

Figure S7. An $AE_{550\text{-}865}$ evaluation of CTL_{ECHAM} (a,b) and DAS_{ECHAM} (c,d) against AERONET. In the maps the inner circle depicts the mean $AE_{550\text{-}865}$ of all AERONET stations within a grid cell of the model while the outer circle depicts the difference between experiments minus AERONET. The size of the points is analogous to the number of the available data points in each case. The scatterplots use all the available data points of the displayed stations.

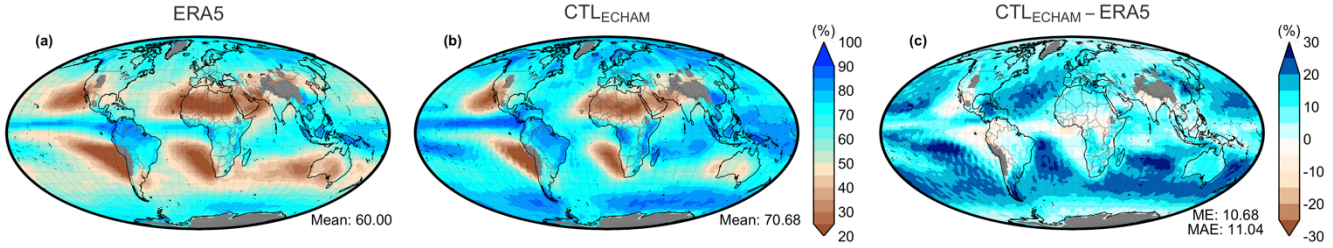

Figure S8. The relative humidity of (a) ERA5 used for aerosol water growth in CTL_{ERA5}, (b) CTL_{ECHAM} and the difference (c) CTL_{ECHAM} – ERA5 for 2006 at 800hPa. The global mean, the global mean error (ME) and the global mean absolute error (MAE) is depicted at the right bottom corner of each plot.